Portable Coherent Frequency-Modulated Continuous-Wave Radar for Indoor Human Tracking

Zhengyu Peng[1], José-María Muñoz-Ferreras[2], Yao Tang[1], Roberto Gómez-García[2], and Changzhi Li[1]
[1]Dept. Electrical & Computer Engineer., Texas Tech University, Lubbock, TX 79409, USA
[2]Dept. Signal Theory & Commun., University of Alcalá, Alcalá de Henares, 28871, Madrid, SPAIN

***Abstract*— Radar-based human tracking can be applied to indoor healthcare scenarios, such as fall detection of elderly people. In this work, a portable frequency-modulated continuous-wave (FMCW) radar prototype for indoor human tracking is presented. The system provides absolute-range detection capabilities. Furthermore, it uses a novel approach—not requiring the sharing of the generation and acquisition clocks—to possess the highly-desired coherence feature, which enables the preservation of the phase history of targets. As a result, videos of inverse synthetic aperture radar (ISAR) images—i.e., videos of range-Doppler frames—can be reconstructed. Experimental results for a walking person in a highly-cluttered indoor environment confirm the suitability of the low-cost radar prototype for indoor healthcare applications.**

***Index Terms*— Coherent radars, frequency-modulated continuous-wave (FMCW) radars, indoor scenarios, inverse synthetic aperture radar (ISAR).**

I. Introduction

The application of radars to indoor scenarios is becoming highly appealing [1]. In particular, Doppler radars have emerged as adequate devices to detect the presence of humans or even to monitor vital signs [2]. An interesting application to improve the quality of life of elderly people is the detection of unfortunate falls [3], [4].

Doppler radars do not possess range resolution—i.e., they do not transmit instantaneous bandwidth—and hence, they cannot obtain absolute ranges of targets. Conversely, they can obtain precise Doppler information related to the target radial velocity [2]. Frequency-modulated continuous-wave (FMCW) radars have recently been proposed for vital-sign monitoring [5]. These systems have range resolution—i.e., they can estimate absolute distances—, leading also to range-bin isolation capabilities [5].

To make an FMCW radar a coherent system is not trivial, since it requires to share the clocks at the generation and acquisition stages [5]. However, if the coherence property for the FMCW radar is achieved, the phase history of targets is preserved during the coherent processing interval (CPI) and Doppler information can thus be derived. This provides the system with two dimensions—i.e., the range and the Doppler—, which can be used to isolate more easily the wanted targets from surrounding clutter.

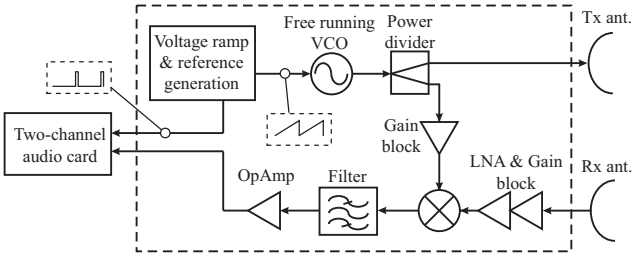

Fig. 1. Simplified block diagram of the portable FMCW radar.

In this work, a low-cost compact coherent FMCW radar prototype is detailed. It works at C-band with a center frequency of 5.8 GHz. A unique feature of the system—beyond its cost and compactness—is that the coherence property is achieved by simultaneously sampling the baseband signal and a reference locked to tuning voltage of the voltage controlled oscillator (VCO). This leads to simplicity in terms of the fact that the generation and acquisition clocks can be different—i.e., the analog-to-digital converter (ADC) can work with its internal clock, that is independent of that of the radar signal generator.

Experimental results—consisting of video frames obtained after applying a method to reconstruct inverse synthetic aperture radar (ISAR) images—enable to verify the coherence of the radar and the possibility to track the echoes of a walking person in the 2D range-Doppler domain for indoor healthcare applications.

II. Description of the Radar Prototype

A high-level architecture for the 5.8-GHz radar prototype is shown in Fig. 1. The dashed box groups together the RF and baseband circuits in two PCB substrates with a total volume of 60mm×50mm×15mm. The transmission (Tx) and reception (Rx) radiation elements are two wideband Vivaldi antennas. The acquisition block is comprised by the audio card in a laptop.

The Tx baseband generation block uses simple operational-amplifier-based electronics to obtain two signals with the same period: a voltage sawtooth signal and a pulsed one—i.e., the reference signal—, to be acquired by the audio card. The voltage sawtooth signal excites a

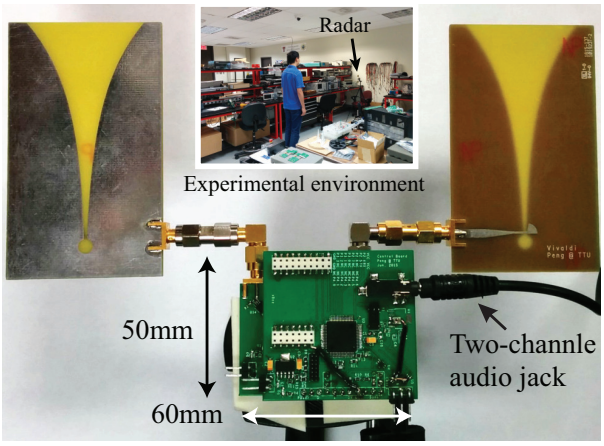

Fig. 2. Photograph of the portable coherent FMCW radar prototype. Inset: Highly-cluttered experimental environment.

TABLE I
PARAMETERS OF THE COHERENT FMCW RADAR PROTOTYPE

Center frequency (f_c)	5.8 GHz
Transmitted bandwidth (B)	300 MHz
Transmitted average power	8 dBm
Waveform period (T)	15.2 ms
Sampling frequency (f_s)	44.1 kHz

free-running VCO which outputs the C-band chirps to be subsequently transmitted. The RX part proceeds with the mixing of a replica of the transmitted signal—which is derived from a power divider—with the received echoes. This is the so-called analog deramping technique [5], giving rise to a narrow-band baseband signal, which can be easily acquired by a low-end ADC—note that the sampling frequency of the audio card is only $f_s = 44.1$ kHz—. Before acquisition, the baseband signal is adequately filtered and amplified, as shown in Fig. 1.

A photo of the low-cost compact radar prototype is provided in Fig. 2. The simultaneous sampling of the reference and baseband signals enables a correct formatting of the baseband-signal samples to construct the raw-data matrix [5]. This is a simple solution which guarantees the coherence of the system, without the necessity of sharing clocks between the generation and acquisition blocks.

The parameters of the radar are detailed in Table I. The chirp rate can be calculated as $\gamma = B/T = 2 \cdot 10^{10}$ Hz/s. The range resolution is given by $\Delta_R = c/(2B) = 0.5$ m, with c being the speed of light. The maximum non-ambiguous range—note that the baseband signal is a real-valued signal—is provided by $R_{\max} = cf_s/(4\gamma) = 165.4$ m. Finally, as widely known, the Doppler frequency is contained in the interval $[-0.5/T, 0.5/T]$, which gives rise to a maximum non-ambiguous velocity for moving targets of $v_{\max} = \lambda/(4T) = 0.85$ m/s, where λ is the wavelength for the transmitted center frequency ($\lambda = c/f_c$).

III. CONSTRUCTION OF THE ISAR VIDEO

As detailed in Section II, the construction of the raw-data matrix is accomplished by detecting the beginning of each ramp with the help of the reference pulsed signal. For each transmitted period T, there are a total of $N = \lfloor T \cdot f_s \rfloor$ fast-time samples. Additionally, the number of slow-time instants is $M = \lfloor CPI/T \rfloor$. Thus, the raw-data matrix $\mathbf{M}_r[m, n]$ has M rows and N columns [5].

Since the range information for a deramping-based FMCW radar is contained in the frequency of the baseband signal, a Fourier transform applied to each row of the raw-data matrix gives rise to the corresponding range-profile matrix—i.e., the range-slow-time map $\mathbf{M}_{rp}[m, q]$, where q is the index to the bins of the fast-time frequency—. The first frame of the ISAR video can be obtained by taking the first M_{chip} range profiles—i.e., $\mathbf{M}_{rp}[m_1, q]$, where $m_1 = \{1, 2, \ldots, M_{chip}\}$ with $M_{chip} \ll M$—and applying to this matrix a column-wise Fast Fourier Transform (FFT). The application of this Fourier transform gives rise to the first frame of the ISAR image—i.e., a range-Doppler matrix—, since the frequency associated with the slow-time is the Doppler frequency [5]. Obtaining the next frames of the ISAR video simply requires taking M_{chip} consecutive range profiles from the complete complex-valued range-slow-time matrix $\mathbf{M}_{rp}[m, q]$ and applying the corresponding column-wise FFT. In this procedure, some of the M_{chip} consecutive range profiles for the current ISAR frame can be overlapped with some of the previous ISAR image, if desired.

To obtain the range profiles and the range-Doppler ISAR frames, the zero-padding technique can be applied both to the fast- and slow-time [5]. As known, this procedure provides more points in the transformed domains, leading to a better estimation of the point spread function (PSF) of targets. To reduce secondary lobes which could mask weak returns from the desired target, conventional windowing—e.g., Hanning weighting—can also be applied.

IV. EXPERIMENTAL RESULTS

The radar prototype was used to illuminate a walking person which was slowly moving away from the radar and then returning back to it. The indoor scenario was a laboratory with many stationary clutter returns—see inset in Fig. 2—. The parameters for the ISAR-video-generation procedure are listed in Table II.

Fig. 3 shows the range-profile matrix $\mathbf{M}_{rp}[m, q]$ for the acquisition. Many vertical strips corresponding to stationary clutter returns can be observed. Also, the echoes from the walking subject are identifiable as tilted returns in this range-slow-time map.

A frame of the ISAR video when the person was walking away from the radar is detailed in Fig. 4(a). As a proof of the coherence feature of the low-cost FMCW radar prototype, the zero-Doppler echoes corresponding to

TABLE II
PARAMETERS FOR ISAR VIDEO GENERATION

Coherent Processing Interval (CPI)	23.1 s
Effective number of fast-time samples (N_{ef})	576
Number of slow-time instants (M)	1528
Reduced number of range profiles (M_{chip})	64
Number of row-wise FFT points	4096
Number of column-wise FFT points	512
Windowing type	Hanning

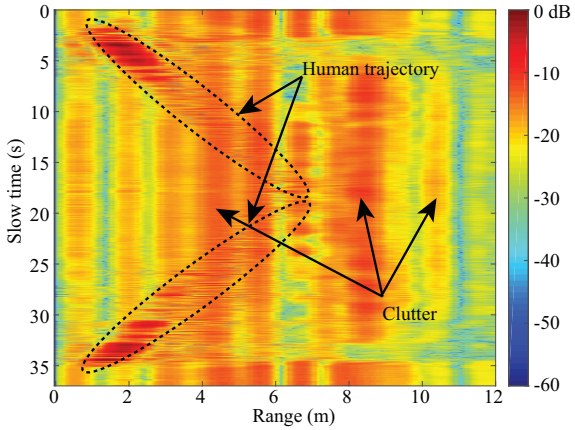

Fig. 3. Range-profile matrix $\mathbf{M}_{rp}[m, q]$ for the experiment.

the stationary clutter are clearly observable. Besides, the echo associated with the person can be seen as a blob in a specific range-Doppler position. The fact of having Doppler information together with the ability of detecting absolute ranges provides the system with 2D isolation and tracking capabilities. This could be leveraged for radar-based indoor healthcare applications.

Fig. 4(b) depicts a frame of the ISAR video when the subject was walking back to the radar. Again, the zero-Doppler returns correspond to the stationary clutter, whereas the moving-target echo has a Doppler frequency with a sign opposite to the result in Fig. 4(a). The echoes observed around the main return in Figs. 4(a) and 4(b) correspond to the micro-Doppler features of the human gait [6].

V. CONCLUSION

The use of a coherent FMCW radar prototype for indoor healthcare applications has been reported. A unique feature of this portable low-cost system is the preservation of the phase/Doppler histories of targets by simultaneously acquiring the baseband and reference signals. Experimental results consisting of inverse synthetic aperture radar (ISAR) video frames have also been demonstrated.

ACKNOWLEDGMENT

This work was supported in part by the National Science Foundation (NSF) under grant ECCS-1254838, the Texas Tech University Global Scholar Academy program, the University of Alcalá under Project CCG-2014/EXP-021, and the Spanish Ministry of Economy and Competitiveness under Project TEC2014-54289-R.

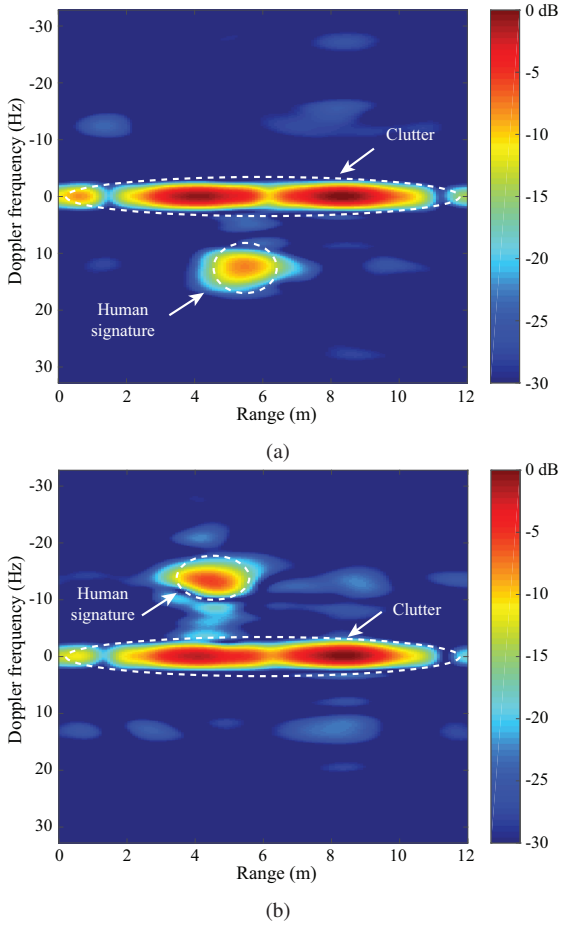

Fig. 4. (a) A frame of the ISAR video when the walking person is moving away from the radar. (b) A frame of the ISAR video when the walking subject is walking back to the radar.

REFERENCES

[1] J. M. Muñoz-Ferreras, Z. Peng, R. Gómez-García, G. Wang, C. Gu, and C. Li, "Isolate the clutter: Pure and hybrid linear-frequency-modulated continuous-wave (LFMCW) radars for indoor applications," *IEEE Microw. Mag.*, vol. 16, no. 4, pp. 40–54, May 2015.

[2] C. Li, V. M. Lubecke, O. Boric-Lubecke, and J. Lin, "A review on recent advances in Doppler radar sensors for noncontact healthcare monitoring," *IEEE Trans. Microw. Theory Techn.*, vol. 61, no. 5, pp. 2046–2060, May 2013.

[3] M. Mercuri, D. Schreurs, and P. Leroux, "SFCW microwave radar for in-door fall detection," in *Proc. IEEE Topical Conf. Wireless Sensors Sensor Networks (WiSNet)*, Santa Clara, CA, USA, Jan. 2012, pp. 53–56.

[4] L. Liang, M. Popescu, M. Rantz, and M. Skubic, "Fall detection using Doppler radar and classifier fusion," in *Proc. IEEE-EMBS Int. Conf. Biomedical Health Informatics*, Hong Kong, China, Jan. 2012, pp. 180–183.

[5] G. Wang, J. M. Muñoz-Ferreras, C. Gu, C. Li, and R. Gómez-García, "Application of linear-frequency-modulated continuous-wave (LFMCW) radars for tracking of vital signs," *IEEE Trans. Microw. Theory Techn.*, vol. 62, no. 6, pp. 1387–1399, Jun. 2014.

[6] V. C. Chen, *The Micro-Doppler Effect in Radar*. Norwood, MA, USA: Artech House, 2011.